

amplified-spontaneous emission (ASE) noise resulting from the amplification process. The probe was combined with the pump signal through a 3-dB fiber coupler. The combined beam was free-space launched into the 2.1-m-long SF57-HF with a coupling efficiency of $\sim 27\%$. The average powers of the pump and probe signals at the input of the fiber were then 17.6 and 13.0 dBm, respectively.

The fiber employed in the experiment was fabricated from the commercial lead-silicate Schott glass SF57 using the structured-element stacking technique (SEST), which allows for the realization of designs with novel dispersion properties. The design and fabrication of this fiber was reported in [8]. The core diameter of the fiber, as obtained from scanning electron microscope images, was $\sim 4.3 \mu\text{m}$. The propagation loss and the nonlinear coefficient γ of the fiber were determined experimentally to be 3.2 dB/m and $164 \text{ W}^{-1} \cdot \text{km}^{-1}$, respectively [9]. The ability of the fiber to maintain linear polarization was also tested. By launching light on one of the principal polarization axes of the SF57-HF, we measured an extinction ratio of ~ 22 dB between the signals received on the two orthogonal polarization axes at the output of the fiber. The beat length of the fiber was experimentally determined to be ~ 0.6 cm, yielding a differential group delay (DGD) of 0.86 ps/m. From separate experiments on four-wave mixing in this fiber, we estimated a zero-dispersion wavelength of 1582 nm and a dispersion slope of $0.2 \text{ ps/nm}^2 \cdot \text{km}$ within the *C*-band [9]. This combination of a low dispersion (with a relatively low dispersion slope), high effective nonlinearity, and good polarization-maintaining properties, makes this SF57-HF ideal for KS applications.

The arrangement of our KS followed the standard configuration. Two polarization controllers at the pump and probe ports were used for adjustment of the state of polarization of the two beams. The polarization of the pump beam was aligned to one of the principal polarization axes of the fiber, while the probe beam was linearly polarized at the SF57-HF input at 45° relative to the pump. The presence of the pump pulses induced an intensity-dependent rotation of the state of polarization of the probe beam. At the output of the SF57-HF, the pump was filtered from the probe using a 3-nm BPF and subsequently, the probe signal passed through two successive amplification and polarization-filtering stages, each consisting of a polarization controller, an EDFA, a BPF, and a polarizer. The polarizers ensured that the Kerr-induced polarization rotation of the probe was transformed into intensity modulation. This was achieved by adjusting the polarization controllers at the input, so that transmission of the probe through the polarizers was minimized in the absence of the pump. The output power of each EDFA was ~ 9.0 dBm. It should be noted that the two successive stages of polarization-filtering the signal were necessary, since the polarizers employed in our setup had a limited extinction ratio of 24 and 18 dB, respectively. The BPFs used in these stages ensured that both the ASE of the two EDFAs and the pump signal were further suppressed. Thus, the pump was effectively suppressed at the output of our system.

III. EXPERIMENTAL RESULTS AND DISCUSSION

The received spectrum at the output of the SF57-HF is shown in Fig. 2(a). Clear sidebands arising from XPM are observed at the probe wavelength. For comparison, the probe spectrum at the input is also shown. In Fig. 2(b), the received spectra after

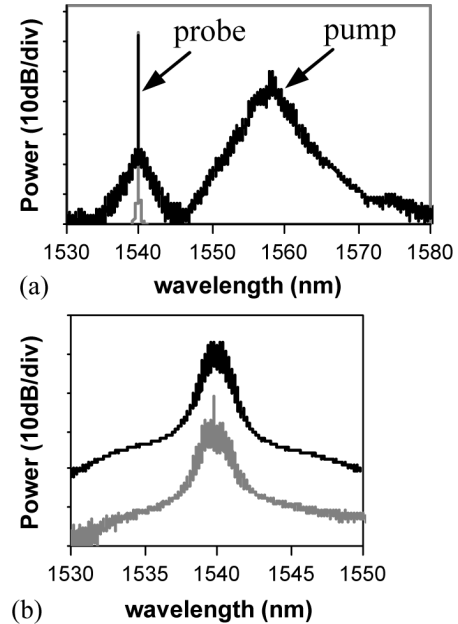


Fig. 2. (a) Spectrum after the SF57-HF when both the pump and the probe are launched (black trace) and input probe spectrum (gray trace); (b) received spectra after the first polarizer (gray trace) and at the output of the system (black trace).

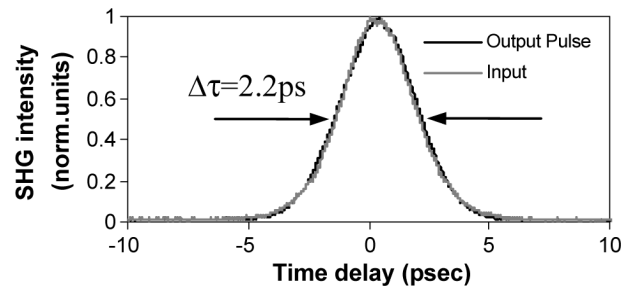


Fig. 3. SHG autocorrelation traces of the input and output pulses of the KS.

each of the two polarizers are shown. It is evident that effective suppression of the CW component of the probe was achieved after the combination of the two polarizers.

We next measured the pulsewidth at the output of the KS through second-harmonic generation (SHG) autocorrelation measurements, and compared it against the width of the input laser pulses (Fig. 3). No pulse broadening was observed, and a pulse FWHM of 2.2 ps was measured at the output. Numerical simulations performed on the KS system, for which the dispersive, nonlinear, and DGD properties of the SF57-HF were taken into account, confirmed this short switching window. This can be understood by considering the combination of the low dispersion of the fiber, which did not lead to substantial broadening of the gating pulse, and its low dispersion slope, which yields a walk-off length of ~ 12 m, i.e., much larger than the physical length of the SF57-HF. (Note that, even if the wavelength separation between the pump and probe had been 30 nm, the walk-off length would be 6 m). The significance of these figures can be appreciated when compared to the values exhibited by other SG-HNLFs. For example, the walk-off length of a step-index bismuth-oxide fiber, similar to the one used in [5], [10] would be just ~ 30 cm for the same conditions

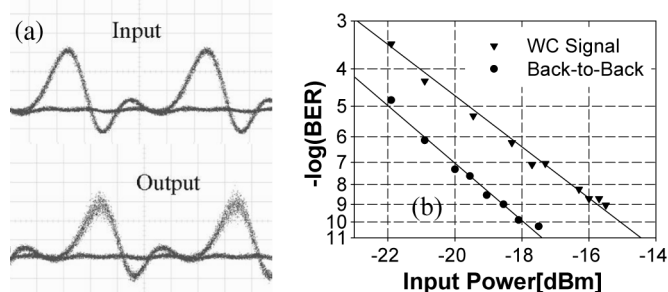


Fig. 4. (a) Eye diagrams of the input and output pulses; (b) corresponding BER curves.

as those considered in our experiment, and the pulsewidth at the output would inevitably be broadened in KS devices of a similar length to those considered here. (This pulse broadening has actually been experimentally observed in [5].) A comparison with conventional germanosilicate HNL technology is not as straightforward. The high degree of control of dispersion and dispersion slope offered by this mature technology means that walk-off issues and the effects of dispersion can largely be eliminated. However, due to the relatively low nonlinear coefficient of conventional HNLs, far longer fiber lengths are in general required, with implications on the effects of environmental stability and latency of the switching system.

The performance of the SF-57-HF wavelength converter was assessed both in terms of eye diagrams and bit-error-rate (BER) tests. In Fig. 4(a), the eye diagrams obtained at the input of the system are compared to the received eye diagrams at the output of the KS. A clear converted eye diagram is observed, albeit with some intensity noise, which we attribute to the accumulation of ASE through the two amplification stages at the output of the system. The effects of ASE are also present in the BER tests shown in Fig. 4(b). The WC process has introduced a power penalty of ~ 3 dB at a BER of 10^{-9} . However, some power leakage from the original CW probe could also be associated with the observed power penalty. Note that the normal dispersion of the SF57-HF at the operating wavelengths discourages the development of any modulation instability effects that might affect the inherent noise performance of the KS.

The SEST fabrication technique allows the implementation of dispersion-optimized soft-glass HF designs that exhibit even higher values of γ than the fiber used in these experiments. Furthermore, even lower values of dispersion and dispersion slope within the C-band are possible [9], thus enabling a further reduction in the achievable length of the switching windows. In addition, previous fabrication attempts [11] have revealed that losses as low as 2 dB/m should readily be achievable in this glass, further reducing the requirements in terms of device length/switching power. Finally, the optical signal-to-noise ratio in our experiments has been severely compromised by the nonoptimum light coupling into and out of the SF57-HF. It is expected that more thorough elaboration on the coupling between the SF57-HF and the SMF patch-cords will greatly improve the noise performance in future KS configurations.

IV. CONCLUSION

A KS operating at 10 Gb/s in the 1.55- μm window and utilizing just 2.1 m of a dispersion-shifted SF57-HF was demonstrated. The combination of a short fiber length and a low dispersion results in a walk-off-insensitive performance, allowing for short switching windows to be realized. The fabrication of our fiber benefited from the SEST technique, which allows sophisticated microstructure designs to be implemented using simple extrusion processes for the fabrication of the preform. We believe that this experiment highlights the potential of soft-glass HF technology for the realization of compact and ultrafast nonlinear devices.

ACKNOWLEDGMENT

The authors wish to acknowledge the contribution of Prof. T. M. Monro and Dr. H. Ebendorff-Heidepriem to the development of the SEST fabrication technique.

REFERENCES

- [1] J. M. Dziedzic, R. H. Stolen, and A. Ashkin, "Optical Kerr effect in long fibers," *Appl. Opt.*, vol. 20, pp. 1403–1406, 1981.
- [2] G. Meloni, M. Scaffardi, P. Ghelfi, A. Bogoni, L. Potì, and N. Calabretta, "Ultrafast all-optical ADD-DROP multiplexer based on 1-m-long bismuth oxide-based highly nonlinear fiber," *IEEE Photon. Technol. Lett.*, vol. 17, no. 12, pp. 2661–2663, Dec. 2005.
- [3] S. Watanabe, R. Okabe, F. Futami, R. Haindberger, C. Schmidt-Langhorst, C. Schubert, and H. G. Weber, "Novel fiber Kerr-switch with parametric gain: Demonstration of optical demultiplexing and sampling up to 640 Gb/s," presented at the Eur. Conf. Optical Communication, Stockholm, Sweden, Sep. 5–9, 2004, Paper Th4.1.6.
- [4] M. Asobe, T. Kanamori, and K. Kubodera, "Applications of highly nonlinear chalcogenide glass fibers in ultrafast all-optical switches," *IEEE J. Quantum Electron.*, vol. 27, no. 8, pp. 2325–2332, Aug. 1993.
- [5] J. H. Lee, K. Kikuchi, T. Nagashima, T. Hasegawa, S. Ohara, and N. Sugimoto, "All-fiber 80-Gbit/s wavelength converter using 1-m-long bismuth oxide-based nonlinear optical fiber with a nonlinearity γ of $1100 \text{ W}^{-1} \cdot \text{km}^{-1}$," *Opt. Express*, vol. 13, pp. 3144–3149, 2005.
- [6] G.-W. Lu, L.-K. Chen, C.-K. Chan, and C. Lin, "All-optical tunable wavelength conversion based on cross-polarisation modulation in nonlinear photonic crystal fibre," *Electron. Lett.*, vol. 41, pp. 203–205, 2005.
- [7] J. H. Lee, T. Nagashima, T. Hasegawa, S. Ohara, N. Sugimoto, and K. Kikuchi, "Wide-band tunable wavelength conversion of 10-Gb/s non-return-to-zero signal using cross-phase-modulation-induced polarization rotation in 1-m bismuth oxide-based nonlinear optical fiber," *IEEE Photon. Technol. Lett.*, vol. 18, no. 1, pp. 298–300, Jan. 1, 2006.
- [8] J. Y. Y. Leong, S. Asimakis, F. Poletti, P. Petropoulos, X. Feng, R. Moore, K. Frampton, T. M. Monro, H. Ebendorff-Heidepriem, W. Loh, and D. J. Richardson, "Towards zero dispersion highly nonlinear lead silicate glass holey fibres at 1550 nm by structured-element-stacking," presented at the Eur. Conf. Optical Communication, Glasgow, U.K., Sep. 25–29, 2005, Paper Th4.4.5, (postdeadline).
- [9] S. Asimakis, P. Petropoulos, F. Poletti, J. Y. Y. Leong, R. C. Moore, K. E. Frampton, X. Feng, W. H. Loh, and D. J. Richardson, "Towards efficient and broadband four-wave-mixing using short-length dispersion tailored lead silicate holey fibres," *Opt. Express*, vol. 15, pp. 596–601, 2007.
- [10] F. Parmigiani, S. Asimakis, N. Sugimoto, F. Koizumi, P. Petropoulos, and D. J. Richardson, "2R regenerator based on a 2-m-long highly nonlinear bismuth oxide fiber," *Opt. Express*, vol. 14, pp. 5038–5044, 2006.
- [11] J. Y. Y. Leong, P. Petropoulos, J. H. V. Price, H. Ebendorff-Heidepriem, S. Asimakis, R. C. Moore, K. E. Frampton, V. Finazzi, X. Feng, T. M. Monro, and D. J. Richardson, "High-nonlinearity dispersion-shifted lead-silicate holey fibers for efficient 1- μm pumped supercontinuum generation," *J. Lightw. Technol.*, vol. 24, no. 1, pp. 183–190, Jan. 2006.